On the Influence of Surface Topography on the Electric Double Layer Structure and Differential Capacitance of Graphite/Ionic Liquid Interfaces

ARTICLE *in* JOURNAL OF PHYSICAL CHEMISTRY LETTERS · SEPTEMBER 2011

Impact Factor: 7.46 · DOI: 10.1021/jz200879a

5 AUTHORS, INCLUDING:

Jenel Vatamanu
University of Utah
38 PUBLICATIONS **857** CITATIONS
SEE PROFILE

Liulei Cao
University of Utah
1 PUBLICATION **63** CITATIONS
SEE PROFILE

Oleg Borodin
Army Research Laboratory
182 PUBLICATIONS **4,079** CITATIONS
SEE PROFILE

Dmitry Bedrov
University of Utah
164 PUBLICATIONS **3,108** CITATIONS
SEE PROFILE

THE JOURNAL OF PHYSICAL CHEMISTRY Letters

LETTER

pubs.acs.org/JPCL

On the Influence of Surface Topography on the Electric Double Layer Structure and Differential Capacitance of Graphite/Ionic Liquid Interfaces

Jenel Vatamanu,*[,†] Liulei Cao,[†] Oleg Borodin,[‡] Dmitry Bedrov,[†] and Grant D. Smith[†]

[†]Department of Materials Science and Engineering, University of Utah, 122 South Central Campus Drive, Salt Lake City, Utah 84112, United States

[‡]Electrochemistry Branch, Army Research Laboratory, 2800 Powder Mill Road; Adelphi, Maryland 20783, United States

Supporting Information

ABSTRACT: Molecular simulations reveal that the shape of differential capacitance (DC) versus the electrode potential can change qualitatively with the structure of the electrode surface. Whereas the atomically flat basal plane of graphite in contact with a room-temperature ionic liquid generates camel-shaped DC, the atomically corrugated prismatic face of graphite with the same electrolyte exhibits bell-shaped behavior and much larger DCs at low double-layer potentials. The observed bell-shaped and camel-shaped DC behavior was correlated with the structural changes occurring in the double layer as a function of applied potential. Therefore, the surface topography clearly influences DC behavior, suggesting that attention should be paid to the electrode surface topography characterization in the studies of DC to ensure reproducibility and unambiguous interpretation of experimental results. Furthermore, our results suggest that controlling the electrode roughness/structure could be a route to improving the energy densities in electric double-layer capacitors.

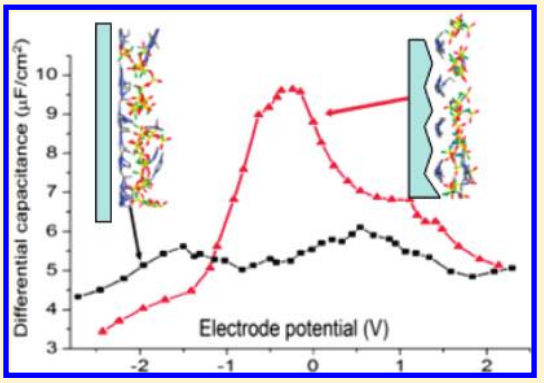

SECTION: Surfaces, Interfaces, Catalysis

Understanding the behavior of the differential capacitance (DC) as a function of the electrode potential is essential to improving the energy density of electric double-layer (EDL) capacitors. Knowledge of the double-layer structure and electrolyte species in direct contact with the electrode is also important for identifying pathways for charge transfer from the electrode to electrolyte that occurs during solid electrolyte interphase formation in lithium ion batteries. Connection of the DC to the EDL structure is a central point to many EDL models, from the simple Gouy−Chapman[1] approximation to the more recent and sophisticated Kornyshev[2] formulation or Lamperski et al. treatment.[3] As originally defined in ref 2, the dependence of DC on the applied potential can be either camel- (or U-) shaped,[4] having a minimum near the potential of zero charge (PZC) flanked by two maxima at larger potentials, or bell-shaped,[5] with one single maximum at a relatively low applied potential. The reasons behind the qualitatively different dependence of DC on electrode potential for different electrode/electrolyte combinations are only partially understood. Kornyshev demonstrated that excluded volume steric interactions and the electrolyte compressibility within the double layer can play a major role in determining DC shape, that is, high compressibility of ionic liquid within the EDL could result in a faster extent of electrolyte accumulation near the surface, thus promoting U-shaped DC.[2] A U-shaped DC is favored on a weakly populated electrode surface[2] and at low temperature because of low free-energy penalty for adding ions from solution to the EDL;[3] conversely, high densities and high temperatures favor bell-shaped DC. The shape, chemical structure, and size of electrolyte ions have a significant impact on the shape of DC. Fedorov et al.[6,7] and we[8] showed that the replacement from surface of neutral or weakly charged tails (denoted by the Fedorov as "latent voids") with strongly charged ones promotes camel-shaped DC.

Although the influence of temperature, density,[9] electrolyte polarizability,[10] and dispersion interactions[11] on DC for room temperature ionic liquid electrolytes is beginning to be understood, the role of the electrode surface structure on DC is unclear and perhaps controversial. Islam et al.[12] reported for [*N*,*N*-diethyl-*N*-methyl-*N*-(2-methoxyethyl) ammonium][bis(trifluoromethylsulfonyl) imide] (TFSI) bell-like DC on Pt and Au electrodes and a U-shaped DC for glassy carbon electrodes. In contrast, Lockett at al.[13] found similarity between shapes of DCs for [1-butyl-3-methylimidazolium(bmim)][PF_6] on both polycrystalline metals (Au and Pt) and glassy-carbon electrodes, concluding that for these systems the nature of electrode surface does not

Received: June 29, 2011
Accepted: August 16, 2011
Published: August 16, 2011

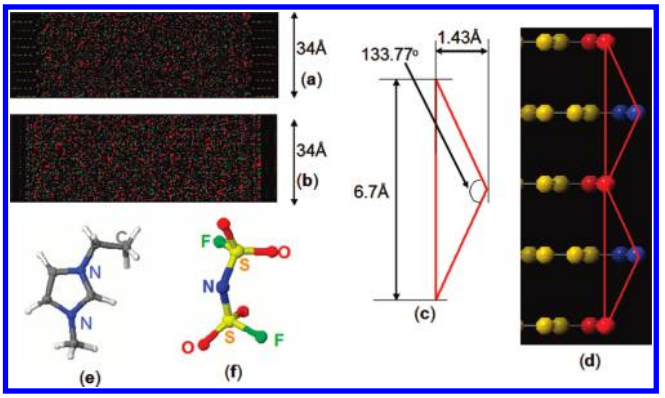

Figure 1. Snapshots of simulation cell for (a) the rough and (b) flat surfaces. (c) Schematic representation of the surface roughness for the prismatic graphite surface. (d) Snapshot of the rough graphite surface corresponding to the geometry in part c. Structure of the (e) emim cation and (f) FSI anion.

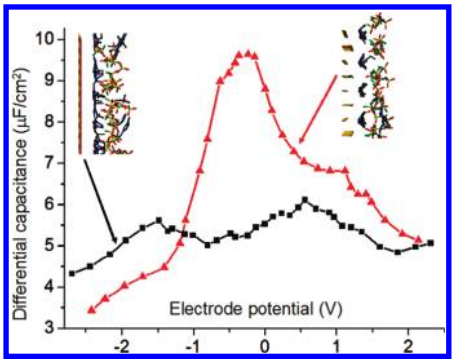

Figure 2. Differential capacitance as a function of EDL potential for flat and rough electrode surfaces. Inserted are image snapshots indicating the electrolyte structure near flat (left insert) and rough (right insert) surfaces at ~2.5 V.

significantly alter the shape of DC curves. Interestingly, the quite different DC behavior for similar ILs reported Lockett at al.[13] and Islam et al.[12] was attributed to the difference in the structure of the glassy carbon electrodes due to different thermal history. In contrast with these findings, Lockett at al.[14] also reported that DC curves vary little on crystalline and noncrystalline electrodes in an imidazolium chloride electrolyte. The variability of DC results for poorly prepared polycrystalline electrodes,[15] on the other hand, indicates a dependence of DC and of EDL structure on the crystallographic orientation of the electrode surface. A recent study by Su et al.[16] of EDL structure formed by $bmim^+$ cation and BF_4^- or PF_6^- anions on a single crystal Au[001] electrode surface showed a strong dependence on changes in the surface topography upon surface reconstruction of the adsorbed $bmim^+$ ordering near the surface and suggested a significant impact of surface orientation on the innermost EDL structure and DC.

In this work, we demonstrate that the atomic-scale topography of the electrode surface can qualitatively change the shape of DC, especially near the PZC. Specifically, our molecular dynamics (MD) simulations demonstrate that an ionic liquid in contact with the atomically flat (basal) crystallographic face of graphite generates a camel-shaped DC, whereas the same electrolyte in contact with atomically corrugated prismatic face of graphite generates a bell-shaped DC.

The simulation setup consisted of an ionic liquid (IL) inserted between two graphite electrodes. The successive hexagonal graphite layers were stacked in ABAB sequence. Snapshots of the simulation cell showing the specific electrode surface orientation toward electrolyte are given in Figure 1a,b.

The basal plane electrode will be referred to as the "flat" electrode, and the prismatic edge electrode will be referred to as the "rough" electrode throughout this Letter. A cartoon of the rough surface showing the "bump" of ~1.43 Å and the corresponding angle of the prism of 133.77° is shown in Figure 1c,d. The IL consists of 1-ethyl-3-methyl imidazolium (emim) and bis-fluorosulfonyl imide (FSI) with a low concentration of LiFSI. The simulated system contained 240 $emim^+$, 310 FSI^-, and 70 Li^+ ions. The chemical structures of cation and anion are shown in Figure 1e,f and are representative of ILs commonly investigated for EDL capacitor applications. The interactions between ions were modeled using a nonpolarizable version of the APPLE&P force field[17] reported previously to reproduce well the bulk properties of RTILs.[18]

The box size along the z direction was adjusted to yield bulk density in the middle of the simulation box. The temperature was controlled with a Nosé–Hoover thermostat.[19] The short-ranged interactions (dispersions and real space Ewald) were evaluated within a spherical cutoff of 10 Å, and the reciprocal part of Ewald summation was evaluated with computationally expedient SPME (smooth particle mesh Ewald) adapted for 2D periodic geometry.[20]

The polarization of the electrode surface was accounted for with a flexible-charge approach in which the potential difference between electrodes was controlled by minimizing the total electrostatic energy of the system with respect to the electrode charges, as described in refs 21 and 22. Hence, we treated the surface as a highly polarizable conductor set at a desired electrostatic potential. This methodology correctly reproduces the charge distribution on highly conductive surfaces, and it is particularly important for assigning the charge distribution on the rough electrode due to the fact that not all surface atoms are equivalent. MD simulations were performed at 16 potentials at 393 K and at 8 potentials at 453 K ranging between 0 and 7 V.

The equations of motion were integrated with a reversible multitime-step algorithm (RESPA).[23] A time step of 0.5 fs was used for bonding, bending, dihedral, and out-of-plane deformation motions, whereas a 2.5 fs time step was used for nonbonded interactions within a cutoff radius of 7.5 Å. The nonbonded interactions in the range between 7.5 and 10.0 Å and reciprocal part of electrostatic interactions were updated every 5 fs. The electrode charges were updated every 0.25 ps. The cross-section of the simulation cell was 29.9 × 34.5 $Å^2$ for the basal graphite and 34.5 × 33.5 $Å^2$ for prismatic graphite. The distance between the electrodes was large enough to ensure sufficient separation between the electrodes, that is, 100.2 and 88.3 Å for the flat and, respectively, rough surfaces, at 393 K. The simulation trajectory of 48 ns was generated at each applied potential.

The PZC was calculated from the potential drop within the EDL for uncharged electrodes. For the systems at 393 K, the PZC was −0.195 and −0.266 V for the flat and rough electrode, respectively, whereas at 453 K, the corresponding PZCs were −0.200 and −0.270 V. In this work, we define the electrode potential as the potential drop within EDL relative to the PZC, $U_{RPZC} = U_{EDL} - PZC = U_{electrode} - U_{bulk} - PZC$. The EDL potentials were calculated by integrating the plane-averaged (in the x and y directions) 1-D Poisson equation for the charge

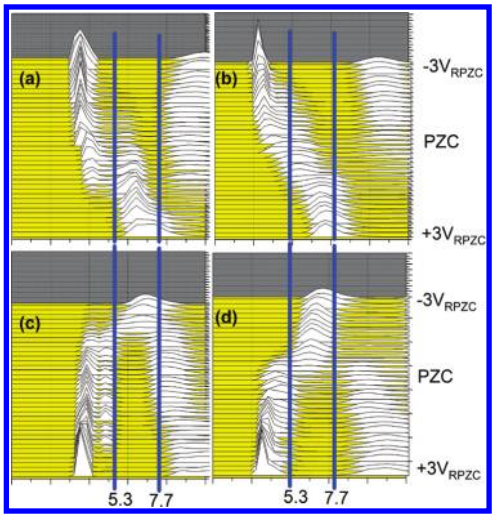

Figure 3. emim cation density profiles as a function of EDL potential for (a) flat surface and (b) rough surface. The FSI cation density profiles as a function of EDL potential for (c) flat surface and (d) rough surface. For the flat surface, the position of the electrode was defined as the center of mass of the outer graphene sheet that is in contact with electrolyte. For the rough electrode, the position of the electrode surface was defined such that the position of the peaks in density profiles roughly coincided with the corresponding peaks at the flat surface. The vertical lines indicate division into the inner Helmholtz layer (<5.3 Å from the surface) and outer Helmholtz layer (between 5.3 and 7.7 Å).

density profiles obtained from simulations along the direction normal to electrode surface. The DC was obtained by fitting a parabola over the local dependence of the electrode charge versus potential using the method described in ref 24 and further confirmed with fitting higher (fourth and fifth) order polynomials over extended potential range.

The dependence of DC on electrode potential for the flat and rough electrodes at 393 K is shown in Figure 2.

The DC curves are qualitatively different for the two graphite surface orientations. Specifically, a camel-shaped DC with a minimum at around $-0.8V_{RPZC}$ and two maxima at $-1.5V_{RPZC}$ and $+0.6V_{RPZC}$ is observed for the IL in contact with the atomically flat basal plane of graphite, whereas a bell-shaped DC with a maximum at $-0.3V_{RPZC}$ is observed in simulations with the prismatic edge of graphite. The DC near PZC is significantly larger (almost double) for the rough electrode compared with the IL | basal plane. For example, at the potential of $-0.3V_{RPZC}$,the DC is 9.6 μF/cm^2 for the rough electrode and 5.6 μF/cm^2 for the flat one. (See Figure 2.) The simulations at 453 K exhibit the same qualitative trend of DC versus electrode potential.

The camel-shaped DC observed on the flat graphite electrodes is not surprising because this electrolyte is similar in structure to *N*-methyl-*N*-propylpyrrolidinium bis(trifluoromethanesulfonyl)imide ([pyr$_{13}$][TFSI])[8] and *N*-methyl-*N*-propylpyrrolidinium bis(fluorosulfonyl)imide ([pyr$_{13}$][FSI]),[25] for which we previously observed a camel-shaped DC at similar temperatures. In those works, the camel-shaped DC was attributed to the ion rearrangement within the EDL double layer upon changing electrode potential.[8] However, it is striking that the shape of DC changes qualitatively from camel-shaped (or U-shaped) to bell-shaped if the flat electrode is replaced with the atomically rough prismatic plane, especially because the degree of surface roughness is small; that is, for the rough surface, the distance between innermost and outermost atoms next to electrolyte is only 1.43 Å. To understand this phenomenon better, we have conducted a detailed analysis of the EDL structure as a function of potential, as represented by the ion center of mass density profiles shown in Figure 3. On the basis of these density distributions, we define (for convenience of discussion) layers of EDL as follows: (i) an inner Helmholtz layer located within 5.3 Å from the electrode surface that encompasses ions adsorbed on the electrode surface, (ii) an outer Helmholtz layer located between 5.3 and 7.7 Å from the electrode surface, and (iii) a second layer located between 7.7 and 10.2 Å from the electrode. It can be seen for both flat and rough electrodes that at high negative and positive voltages the inner Helmholtz and second layers are occupied primarily by counterions, whereas the outer Helmholtz layer is occupied by co-ions (same charge sign as the electrode). Whereas structure in the electrolyte propagates several additional layers away from the electrode, particularly at high electrode potentials,[8,25] understanding the behavior of ions within the Helmholtz layers and the second layer as a function of electrode potential appears to be sufficient to gain qualitative insight into differences in DC exhibited by the flat and rough electrodes, as discussed below.

As EDL potential changes sign (going from large positive to large negative or vice versa), the co-ions move from the inner Helmholtz layer to the outer Helmholtz layer, whereas counterions move in the opposite direction for both flat and rough surfaces. However, there are clear differences in the rate (with changing potential) at which ions rearrange between layers for the two surfaces. The most striking is difference observed for the FSI^- density profiles in the region between PZC and $-1V_{RPZC}$, as shown in Figure 3c,d. In this region, most FSI anions move out from the inner Helmholtz layer at the rough electrode while there remains a large FSI population in the inner Helmholtz layer for the potential range at the flat electrode. The FSI anions do not significantly populate the outer Helmholtz layer at the flat electrode until the potential is more negative than $-1.5V_{RPZC}$. The described pattern of the negative charge desorption with decreasing potential is consistent with a higher DC on the rough surface in the region from -1 to $0V_{RPZC}$ and lower DC for this surface at potentials below $-1.5V_{RPZC}$. Examination of the EDL behavior of the positive electrode reveals differences in emim cation desorption (moving from the inner Helmholtz to the outer Helmholtz layers) between the flat and rough electrodes near PZC and at slightly positive potentials. Specifically, for the flat electrode surface, the population of cations in the inner Helmholtz layer is associated with a growing peak in the outer Helmholtz layer, whereas at the rough surface, the cation density profile tends to broaden and shifts to larger distances with increasing electrode potential.

Additional insight into changes of ion distribution within the EDL with potential and nature of the surface can be gained by examining the number of emim cations and FSI anions per unit area of electrode surface in the inner and outer Helmholtz layers, as shown in Figures 4a and 2 from the Supporting Information. In the potential window $-1.0V_{RPZC} < V < +0.4V_{RPZC}$, the changes in emim cation packing in the two layers are very similar for both surfaces. However, the changes of FSI density with potential are more pronounced for the rough surface for both the inner and outer Helmholtz layers. In particular, in the potential range from $0V_{RPZC}$ to $-1.0V_{RPZC}$, the FSI density in the inner Helmholtz layer decreases much more than observed for the flat electrode, whereas the FSI density in the outer Helmholtz layer increases much more for the rough surface than for the flat one in the same

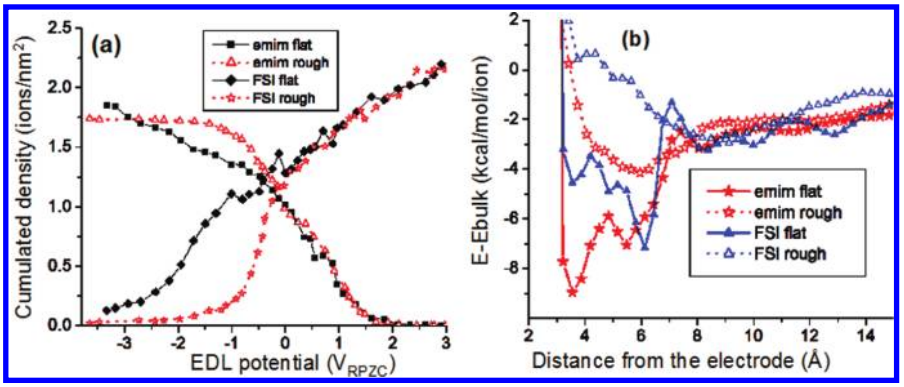

Figure 4. (a) Cumulated number of ions per unit electrode area in the inner Helmholtz layers as a function of electrode potential. The corresponding number of ions per unit electrode surface area in the outer Helmholtz layers as a function of electrode potential is shown in the Supporting Information. (b) Potential energy per ion relative to the bulk ion energy for emim and FSI ions as a function of distance from the electrode.

potential range, in agreement with the above analysis of Figure 3. Therefore, it is likely that the faster FSI displacement from the rough surface with increasing negative potential is an important factor in determining the larger magnitude and the bell-shaped DC on the rough surface. Other features of DC shown in Figure 2 are consistent with the ion density variations with potential in the inner and outer Helmholtz layers. For example, the density of emim in the inner Helmholtz layer and FSI in the outer Helmholtz layer for the rough surface remain essentially constant for potentials more negative than $-1V_{RPZC}$, suggesting faster ion saturation on the negative rough electrode than near the flat one and resulting in a relatively low DC in contrast with the relatively large DC observed on the flat negative surface due to continued increasing emim density at the negative electrode surface, even for potentials lower than $-1V_{RPZC}$. Similarly, at large positive potentials, the density profiles for both ions in both layers show very similar behavior for both surfaces, which is consistent with similar values of DCs obtained for the rough and flat surfaces observed above $+1.7V_{RPZC}$.

Interestingly, the behavior of DC in the potential range 0 to $+0.5V_{RPZC}$ is less clearly correlated with the population of cations and anions in the inner and out Helmholtz layers than for other potentials. Ion populations in this potential range show similar behavior for both surfaces despite quite different behavior of DC. Note, however, that the distribution of cations within the inner and outer Helmholtz layers is quite different in this potential range, as discussed above and shown in Figure 3a,b. Also, the ion distributions in the second layer (Figure 3) indicate faster accumulation rates of the FSI ions near the rough surface compared with the flat electrode. The qualitative trends observable in Figure 4a do not depend on the precise definitions of the layers.

To obtain insight into why EDL structure and DC undergo more dramatic changes at the rough surface than on the flat one with changing potential, particularly near PZC, we compared the intermolecular potential energy for the FSI anion and the emim cation at PZC (where difference in DC between the two systems is large) as a function of the position of the ion center of mass relative to the electrode, as shown in Figure 4b. This energy is the interaction energy of the ion with its environment (electrode + electrolyte) as a function of position relative to the surface. A lower potential energy for an ion near the electrode surface, as is observed for the flat surface compared with the rough, indicates more favorable interactions with the electrode and surrounding electrolyte and is consistent with a larger driving force (e.g., unfavorable electrostatic interactions with the electrode) needed to remove the ion from the surface and hence change the EDL structure. The potential energy of the ions in the inner Helmholtz layer is lower than the corresponding bulk energy by about 5−9 kcal/mol or about 6−11 kT. In contrast, for the rough surface, the intermolecular potential energy for ions in the inner Helmholtz layer is very similar to the bulk energy, indicating that the structure of the rough surface significantly interferes with ability of ions to optimize their structuring in the first two layers. The observed trends in emin and FSI potential energy are consistent with the observed behavior of DC on the rough and flat surface at PZC. Specifically, larger external electric fields are needed to break a more energetically favorable ion packing on the flat surface, resulting in a slower extent of co-ion removal from surface upon changes in electrostatic potential and therefore lower DC. Conversely, the energetically less favorable structure at the rough surface should be less resistant to ion rearrangements under the applied potential, therefore favoring larger DC.

As we mentioned above, the system also contained some Li^+ ions. Our analysis of Li^+ showed no clear correlations with observed features in DCs, likely because of its much lower concentrations (by a factor of 7.85) relative to the cumulated concentration of the other ions. Moreover, our subsequent simulations of different ILs that did not contain Li salts showed qualitatively similar trends in DCs differences between rough and flat electrodes, further confirming that results presented here are more generic to this class of systems.

Finally, it is interesting to note that most of the experimental DCs we used for comparison were obtained with the dynamic "impedance method". In this context, however, the recent work of Kolb[26] should be noted, which suggests the inherent difficulties of this "dynamic" experimental method of DCs measurement and the validity of data interpretation using equivalent circuit construction. In simulations, extraction of DC is straightforward because both the electrode charge and EDL potential drop can be computed directly. We surmise that simulation data such as that presented here can, in principle, be used to validate and calibrate the impendance method, assuming that the equivalent (chemically and structurally) system is investigated in experiment and simulation.

In summary, MD simulations have shown that the atomic level roughness of the electrode surface can qualitatively change the dependence of the DC on the applied potential difference for an

ionic liquid electrolyte. This "roughness" is qualitatively different from that which makes the ions move in a confined geometry of nanopores or a nanotemplated electrode,[27] which was theoretically explained in refs 28 and 29. The impact of surface roughness observed here is explained by a strong dependence of the electrolyte packing within the double layer on the surface topography and by the large differences in intermolecular potential energy of the electrolyte ions near flat and rough surfaces. Our results indicate that interpretation of the experimental DC should also consider detailed knowledge of the electrode surface topography and its roughness, and it should go beyond the typical route of considering the electrolyte behaviors near a flat surface (as done in the most basic EDL model). On the basis of clearly different DCs observed for two surfaces, we suggest that a possible route to improve the energy densities in supercapacitors is to control the roughness of the electrode surface.

The observed behavior reported here accounts for a microscopic sample of the surface. The DC for macroscopic-sized surface would be expected to be an average of the DCs for each individual facet exposed toward the electrolyte. The dynamic processes on the surface that can modify the surface topography, such as the surface reconstruction, would be expected to influence the shape of DC over longer time scales. The possibility that different crystallographic orientations in equilibrium (or close to equilibrium) with liquid phases restructure forming very similar topologies has been previously observed, for example, in ref 30, for a simple fcc crystal/melt interface. It is possible that surfaces that can restructure (such as metallic surfaces) would show a smaller extent or no DC variation with the crystallographic orientation if various crystallographic faces in contact with RTIL form similar surface motifs upon restructuring. Graphite surfaces where atoms are covalently bonded would be expected to exhibits nontrivial dependence of DC on the crystallographic face and its inherent roughness, as shown in this work.

■ ASSOCIATED CONTENT

Supporting Information. Electrode charge versus potential at 393 K, the variation of cumulated ion density in the outer-Helmholtz layer, the electrode charge and DC versus potential at 453 K, and image snapshots of the electrolyte ordering near surface at various potentials. This material is available free of charge via the Internet at http://pubs.acs.org.

■ AUTHOR INFORMATION

Corresponding Author
*E-mail: u0615401@utah.edu.

■ ACKNOWLEDGMENT

We are grateful to U.S. Department of Energy under contract grant DE-SC00019112 and contract no. DE-AC02-05CH11231 on PO no. 6838611 (University of Utah). This research used resources of the National Energy Research Scientific Computing Center, which is supported by the Office of Science of the U.S. Department of Energy under Contract No. DE-AC02-05CH11231.

■ REFERENCES

(1) Bard, A. J.; Faulkner, L. R. *Electrochemical Methods: Fundamentals and Applications*; John Wiley & Sons: New York, 2001.

(2) Kornyshev, A. A. Double-Layer in Ionic Liquids:Paradigm Change? *J. Phys. Chem. B* **2007**, *111*, 5545–5557.

(3) Lamperski, S.; Outhwaite, C. W.; Bhuiyan, L. B. The Electric Double-Layer Differential Capacitance at and near Zero Surface Charge for a Restricted Primitive Model Electrolyte. *J. Phys. Chem. B* **2009**, *113*, 8925–8929.

(4) Silva, F.; Gomes, C.; Figueiredo, M.; Renata, C.; Martins, A.; Pereira, C. M. The Electrical Double Layer at the [BMIM][PF6] Ionic Liquid/Electrode interface — Effect of Temperature on the Differential Capacitance. *J. Electroanal. Chem.* **2008**, *622*, 153–160.

(5) Alam, M. T.; Islam, M. M.; Okijima, T.; Ohsaka, T. J. Electrical Double Layer in Mixtures of Room-Temperature Ionic Liquids. *J. Phys. Chem. C* **2009**, *113*, 6596–6601.

(6) Fedorov, M. V.; Kornyshev, A. A. Towards Understanding the Structure and Capacitance of Electrical Double Layer in Ionic Liquids. *Electrochim. Acta* **2008**, *53*, 6835–6840.

(7) Georgi, N.; Kornyshev, A. A.; Fedorov, M. V. The Anatomy of the Double Layer and Capacitance in Ionic Liquids with Anisotropic Ions: Electrostriction vs. Lattice Saturation. *J. Electroanal. Chem.* **2010**, *649*, 261–267.

(8) Vatamanu, J.; Borodin, O.; Smith., G. D. Molecular Insights into the Potential and Temperature Dependences of the Differential Capacitance of a Room-Temperature Ionic Liquid at Graphite Electrodes. *J. Am. Chem. Soc.* **2010**, *132*, 14825–14833.

(9) Lauw, Y.; Horne, M. D.; Rodopoulos, T.; Leermarks, F. A. M. Room-Temperature Ionic Liquids: Excluded Volume and Ion Polarizability Effects in the Electrical Double-Layer Structure and Capacitance. *Phys. Rev. Lett.* **2009**, *103*, 117801–117804.

(10) Tazi, S.; Salanne, M.; Simon, C.; Turq, P.; Pounds, M.; Madden, P. A. Potential-Induced Ordering Transition of the Adsorbed Layer at the Ionic Liquid/Electrified Metal Interface. *J. Phys. Chem. B* **2010**, *114*, 8453–8459.

(11) Trulsson, M.; Algotsson, J.; Forsman, J.; Woodward, C. E. Differential Capacitance of Room Temperature Ionic Liquids: The Role of Dispersion Forces. *J. Phys. Chem. Letters* **2010**, *1*, 1191–1195.

(12) Islam, M.; Alam, M. T.; Ohsaka, T. Electrical Double-Layer Structure in Ionic Liquids: A Corroboration of the Theoretical Model by Experimental Results. *J. Phys. Chem. C* **2008**, *112*, 16568–16574.

(13) Lockett, V.; Mike, H.; Sedev, R.; Rodopoulos, T.; Ralston, J. Differential Capacitance of the Double Layer at the Electrode/Ionic Liquids Interface. *Phys. Chem. Chem. Phys.* **2010**, *12*, 12499–12512.

(14) Lockett, V.; Sedev, R.; Ralston, J.; Horne, M.; Rodopoulos, T. Differential Capacitance of the Electrical Double Layer in Imidazolium-Based Ionic Liquids: Influence of Potential, Cation Size, and Temperature. *J. Phys. Chem. C* **2008**, *112*, 7486–7495.

(15) Adamson, A. W. *Physical Chemistry of Surfaces*; Wiley: New York, 1997.

(16) Su, Y. Z.; Fu, Y. C.; Yan, J. W.; Chen, Z. B.; Mao, B. W. Double Layer of Au(100)/Ionic Liquid Interface and Its Stability in Imidazolium-Based Ionic Liquids. *Angew Chem. Int. Ed.* **2009**, *48*, 5148–5151.

(17) Borodin, O. Polarizable Force Field Development and Molecular Dynamics Simulations of Ionic Liquids. *J. Phys. Chem. B.* **2009**, *113*, 11463–11478.

(18) Bedrov, D.; Borodin, O.; Li, Z; Smith, G. D. Influence of Polarization on Structural, Thermodynamic, and Dynamic Properties of Ionic Liquids Obtained from Molecular Dynamics Simulations. *J. Phys. Chem. B* **2010**, *114*, 4984–4997.

(19) Hoover, W. G. Canonical Dynamics: Equilibrium Phase-Space Distributions. *Phys. Rev. A* **1985**, *31*, 1695–1697.

(20) Kawata, M.; Mikami, M. Rapid Calculation of Two-Dimensional Ewald Summation. *Chem. Phys. Lett.* **2001**, *340*, 157–164.

(21) Reed, S. K.; Lanning, O. J.; Madden, P. A. Electrochemical Interface between an Ionic Liquid and a Model Metallic Electrode. *J. Chem. Phys.* **2007**, *126*, 084704–13.

(22) Vatamanu, J.; Borodin, O.; Smith, G. D. Molecular Dynamics Simulations of Atomically Flat and Nanoporous Electrodes with a Molten Salt Electrolyte. *Phys. Chem. Chem. Phys.* **2010**, *12*, 170–182.

(23) Martyna, G. J.; Tuckerman, M. E.; Tobias, D. J.; Klein, M. L. Explicit Reversible Integrators for Extended Systems Dynamics. *Mol. Phys.* **1996**, *87*, 1117–1157.

(24) Fedorov, M. V.; Kornyshev, A. A. Ionic Liquid Near a Charged Wall: Structure and Capacitance of Electrical Double Layer. *J. Phys. Chem. B.* **2008**, *112*, 11868–11872.

(25) Vatamanu, J.; Borodin, O.; Smith., G. D. Molecular Simulations of the Electric Double Layer Structure, Differential Capacitance, and Charging Kinetics for *N*-Methyl-*N*-propylpyrrolidinium Bis(fluorosulfonyl)imide at Graphite Electrodes. *J. Phys. Chem. B* **2011**, *115*, 3073–3084.

(26) Gnahm, M.; Pajkossy, T.; Kolb, D. M. The Interface Between Au(111) and an Ionic Liquid. *Electrochim. Acta* **2010**, *55*, 6212–6217.

(27) Largeot, C.; Portet, C.; Chmiola, J.; Taberna, P. L.; Gogotsi, Y.; Simon, P. J. Relation between the Ion Size and Pore Size for an Electric Double-Layer Capacitor. *J. Am. Chem. Soc.* **2008**, *130*, 2730–2731.

(28) Kondrat, S.; Kornyshev, A. A. Superionic State in Double-Layer Capacitors with Nanoporous Electrodes. *J. Phys.: Condens. Matter* **2011**, *23*, 022201.

(29) Kondrat, S.; Georgi, N.; Fedorov, M. V.; Kornyshev, A. A. A Superionic State in Nano-Porous Double-Layer Capacitors: Insights from Monte Carlo Simulations. *Phys. Chem. Chem. Phys.* **2011**, *13*, 11359–11366.

(30) Vatamanu, J.; Kusalik, P. G. Microfaceting and Its Implication in the Nonrandom Stacking in fcc Crystals. *Phys. Rev. B* **2007**, *76*, 035431–035436.